Title

Coevolution of motor cortex and behavioral specializations associated with flight and echolocation in bats

Journal

Current Biology, 32(13)

ISSN

0960-9822

Authors

Halley, Andrew C
Baldwin, Mary KL
Cooke, Dylan F
et al.

Publication Date

2022-07-01

DOI

10.1016/j.cub.2022.04.094

Peer reviewed

Published in final edited form as:

Curr Biol. 2022 July 11; 32(13): 2935–2941.e3. doi:10.1016/j.cub.2022.04.094.

Coevolution of motor cortex and behavioral specializations associated with flight and echolocation in bats

Andrew C. Halley[1,6], **Mary K. L. Baldwin**[1], **Dylan F. Cooke**[2], **Mackenzie Englund**[3], **Carlos Pineda**[3], **Tobias Schmid**[4], **Michael M. Yartsev**[4,5], **Leah Krubitzer**[1,3,7]

[1]Center for Neuroscience, 1544 Newton Ct., University of California, Davis, CA 95618, USA

[2]Biomedical Physiology and Kinesiology, 8888 University Dr E K9625, Simon Fraser University; Burnaby, BC V5A 1S6, Canada

[3]Department of Psychology, 1 Shields Avenue, University of California, Davis, CA 95616 USA

[4]Helen Wills Neuroscience Institute, 175 Li Ka Shing Center, MC#3370, University of California, Berkeley, CA 94720, USA

[5]Department of Bioengineering, Stanley Hall, 306, University of California, Berkeley, CA 94720, USA

[6]Twitter: @evodevoneuro

[7]Lead contact

Summary

Bats have evolved behavioral specializations that are unique among mammals, including self-propelled flight and echolocation. However, areas of motor cortex that are critical in the generation and fine control of these unique behaviors have never been fully characterized in any bat species, despite the fact that bats compose ~25% of extant mammalian species. Using intracortical microstimulation, we examined the organization of motor cortex in Egyptian fruit bats (*Rousettus aegyptiacus*), a species that has evolved a novel form of tongue-based echolocation.[1,2] We found that movement representations include an enlarged tongue region containing discrete subregions devoted to generating distinct tongue movement types, consistent with their behavioral specialization generating active sonar using tongue-clicks. This magnification of the tongue in motor cortex is comparable to the enlargement of somatosensory representations in species with sensory specializations.[3–5] We also found a novel degree of coactivation between the forelimbs and hindlimbs, both of which are involved in altering the shape and tension of wing

Correspondence: lakrubitzer@ucdavis.edu (L.K.).

Author contributions

A.C.H., M.M.Y., L.K. conceived and designed the experiments. A.C.H., M.K.L.B., D.F.C., M.E., C.P., T.S., M.M.Y., L.K. performed the experiments. A.C.H., M.E., C.P. analyzed the data. A.C.H., M.K.L.B., D.F.C., M.E., C.P., T.S., M.M.Y., L.K. wrote and approved the manuscript.

Declaration of Interests

The authors have no competing interests.

membranes during flight. Together, these findings suggest that the organization of motor cortex has coevolved with peripheral morphology in bats to support the unique motor demands of flight and echolocation.

eTOC Blurb

Using ICMS, Halley et al. describe the first motor map in any species of bat. In a species that uses its tongue to echolocate, they find an exceptionally large representation of the tongue. Forelimb movements are most often coupled with hindlimb movements. Together, this suggests that motor cortex in bats is adapted for echolocation and flight.

Graphical Abstract

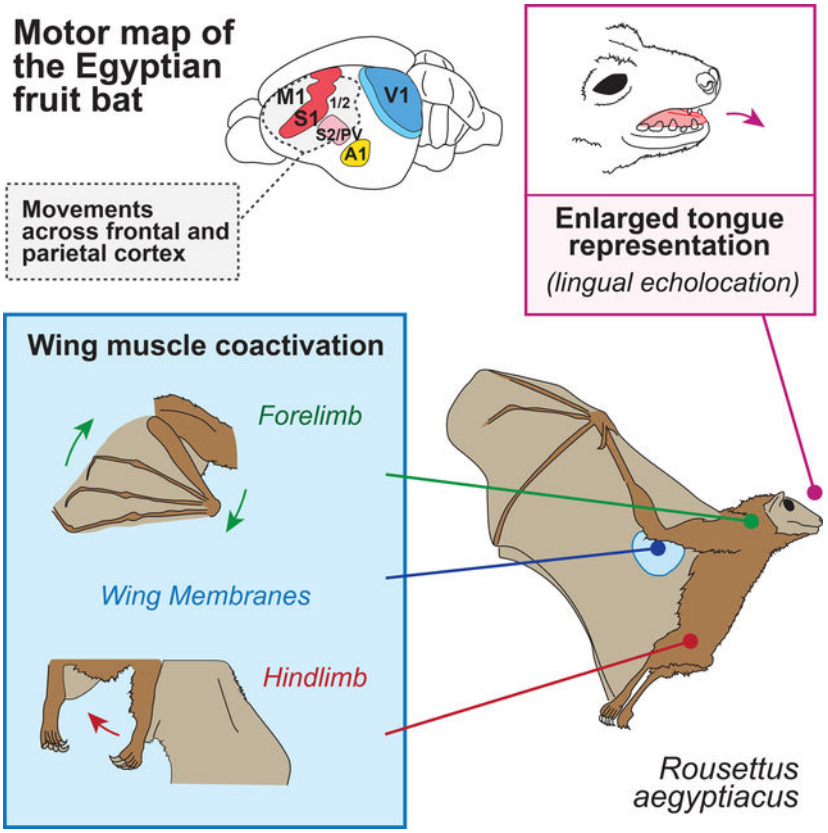

Results and Discussion

In order to characterize the motor cortex of the Egyptian fruit bat, we applied long-train (500ms) intracortical microstimulation (LT-ICMS) to frontal, parietal, occipital, and temporal cortical areas. Electrode sites were directly related to cortical field boundaries in histologically processed tissue (Figure S1). Similar to recent studies in other mammals,[6,7] movements were evoked in motor (M1), somatosensory (S1, S2/PV), and in a parietal region termed area 1/2.[8] Figure 1 shows two representative cases with tail, hindlimb and forelimb movements elicited from caudomedial areas of both M1 and S1, and head/tongue movements elicited from the most rostrolateral portions of S1and the lateral portion of M1

(Figure 1; abbreviations in Table S1; additional cases in Figure S2). Additional hindlimb movements were elicited from area 1/2 and areas S2 and PV. Below we describe the detailed representation of movements associated with these major body parts and general trends in the organization of movement representations in the cortex.

Tongue Movements.

Movements of the tongue were elicited from stimulation of a large and continuous region of caudolateral M1 and rostrolateral S1 (e.g. Figures 1B, 1D) in every case. Tongue movements were relatively rare in other cortical areas (S2/PV in two cases, and absent from area 1/2 in every case). Within the lateral portions of S1, tongue movements were elicited in combination with jaw movements. Along the M1/S1 border, tongue movements were elicited in combination with movements of the nose and upper lip.

We measured the size of tongue representations as a proportion of the other stimulation sites that elicited movement in both S1 and M1 across five cases (see Methods). The average proportion of tongue representations was 40.9% in S1, 43.7% in M1, and 41.5% in S1+M1)(Table 1). Tongue movement types were clustered into distinct territories of S1 and M1 and included twitches of the distal, middle, and proximal tongue (Figure 2A), as well as full extensions of the tongue out of the mouth (Figure 2B). The largest region of this tongue representation included movements of the middle and distal tongue, while proximal (back of the tongue) tongue movements were clustered in two regions. The first representation of the proximal tongue was in a rostromedial region along the S1/M1 border, and movements of the proximal tongue were coupled with movements of the middle and distal tongue, producing extensions of the whole tongue outward (polygons outlined in black in Figure 2A; example case in Figure 2B). The second representation was in caudolateral portion of S1, adjacent to its border with S2/PV. In this representation, proximal tongue movements were frequently observed in isolation, but never as part of a full extension. This distinct representation of tongue movement types, as well as the large amount of cortex that the tongue representation occupies in M1 and S1, are consistent with the precise motor control of the tongue that *Rousettus* exhibits during lingual echolocation,[2] or perhaps other behaviors associated with coordinated tongue use such as frugivory.

Orofacial Movements.

Jaw movements universally involved jaw opening, and were elicited from the lateral portion of S1 in six cases, as well as a distinct medial region along the S1/M1 border in two cases (e.g. Figures 1B, S3A). Nose and upper lip movements were elicited from stimulation of diverse sites across M1, S1, S2/PV, and area 1/2 in three cases (Figures 1B, 1D, S3A). Eyelid movements were observed in five cases, primarily in S2/PV (e.g. Figure 1D), but also in M1 (Figure S2C) and in area 1/2 (not shown). Ear movements were elicited in one case (Figure 1B) from stimulation in S1 and sites caudal to S2/PV.

Forelimb & Hindlimb Movements

Movements of the forelimb were evoked in M1 and S1 in every case (e.g. Figures 1B, D), in S2/PV in four cases (e.g. Figures 1B; S3A), and in area 1/2 in one case (Figure S2C). The majority of forelimb movements that were elicited involved the shoulder (e.g. Figure

2C), while evoked movements of the elbow, wrist and digits were relatively rare. Movements of the shoulder were mostly characterized by lateral movements outward from the midline. Movements of the forelimb digits – primarily an extension of D1 – were evoked from stimulation of M1 or S1 in five cases (e.g. Figure 1D). In one case (not shown), an extension of all the forelimb digits was evoked from two sites – one in S1, and another in M1. Bilateral movements of the forelimb were observed in eight cases, and were primarily elicited from stimulation of more rostral sites, either in M1 or along the M1/S1 border (e.g. in Figure 1B, 3/5 M1 sites, 1/9 S1 sites; in Figure 1D, 14/17 M1 sites, 0/3 S1 sites). In one case (18–145; Figure 1A) bilateral forelimb movements were evoked from stimulation of S2/PV.

Whereas forelimb movements were largely restricted to M1 and S1, hindlimb movements were elicited from a large area of cortex in every case, including M1, S1, S2/PV, and area 1/2. In five cases (e.g. Figure 1B), hindlimb movements were elicited from two distinct regions of cortex, both of which produced movements of the hip, knee, ankle, and toes. The first region of hindlimb movements was observed along an extensive medial aspect of cortex in every case, spanning from area 1/2 through S1 to M1 (e.g. Figures 2, S2B). The second area was observed in five cases, and included hindlimb movements evoked from stimulation of S2/PV (e.g. Figures 1, S3C), though at higher stimulation thresholds. In general, stimulation in more rostral regions (e.g. M1, rostral S1) generated movement of the hindlimb forward and medially, while sites along the caudomedial aspect of S1 and area 1/2 produced retractions of the hindlimb upward or backward. Across M1, S1, 1/2, and S2/PV, flexion was the dominant direction for movements of the hip (moving the hindlimb forward and medially) as well as the knee ankle (bringing the hindlimb upward toward the body).

Membrane and Tail Movements

In four cases, we observed movements of the wing membranes that were distinct from adjacent limb muscles. In two cases (e.g. Figure S2C), we elicited movements of membranes that span between forelimb digits (*dactylopatagium*) during stimulation of sites in S1 and M1. These sites were located rostral and lateral to forelimb sites that elicited digit movements (Figure S2C). In addition, in two different cases during stimulation of area 1/2, we elicited movements of the most caudal membranes that span the midline and connect the hindlimbs (*uropatagium*)(Figures 1B, 1D). These sites were adjacent to ankle, toe, and tail representations. Finally, tail movements were evoked from stimulation of areas S1 and 1/2 in two cases (e.g. Figure 1B); every site produced movements of the tail toward the midline.

Movement Thresholds

The minimal threshold stimulation parameters using long-train stimulation (500 ms) for cases 18–145 and 18–155 are shown in Figure S1, and detailed threshold data based on cortical field location and body parts are described for these two cases in Table S1. On average, movement thresholds were lowest in M1 (82.5 μA) followed by S1 (96.7 μA), S2/PV (145.5 μA) and area 1/2 (185.3 μA). Averaged across cortical areas, the lowest thresholds were observed in the tongue representation (60.7 μA), followed by the forelimb (100.0 μA), hindlimb (129.6 μA) and face representations (136.1 μA). As we might expect, body part representations with the lowest movement thresholds (e.g. tongue) are concentrated in cortical areas with the lowest movement thresholds (e.g. S1, M1).

Discussion

Bats exhibit two interlinked behaviors that are exceptional among mammals: self-propelled flight, and the production of active sonar to echolocate. Both flight and active sonar require a rapid integration of sensory input and motor output. While the sensory basis of echolocation has been studied extensively, little is known about the organization of motor cortex in any bat species. In this study, we produced the first motor map of any bat species. We found that the motor neocortex of the Egyptian fruit bat (*Rousettus aegyptiacus*) is uniquely organized to integrate forelimb and hindlimb movements during flight, and contains an enlarged representation of the tongue, including distinct representations of different tongue regions, to support lingual echolocation.

In bats, flight requires a coordination of muscles across the forelimb, hindlimb, and wing membranes that alter the camber of the wings during flight,[9] a process guided by sensory hairs covering the wing membrane.[10] Previous studies in megabats have shown connections between forelimb and hindlimb regions of sensory and motor areas of neocortex[8] and across hemispheres[11], suggesting that there is a direct and broadly distributed sensorimotor network involved in the coordination of the limbs in the production of flight.

In the present study, stimulation sites that elicited movements of the forelimb were usually coupled with movements of the hindlimb. This coactivation of muscle groups at a single stimulation site is remarkable when compared to other species that have been studied using similar techniques (i.e. LT-ICMS). For example, in *Rousettus*, movements of the forelimb were elicited in combination with movements of the hindlimb in 62–68% of stimulation sites where movement could be elicited (Figure 1B, 1D), compared with 7–8% in a study of laboratory rats using similar methods[7]. In primates such as macaques and capuchin monkeys, the representation of the forelimb (particularly the digits) dominates motor cortex, and synergistic movements of the forelimb and hindlimb are rare (macaque[6]; capuchin[12]). The few digit movements we observed in *Rousettus* were primarily of D1, which bats use to grip during arboreal climbing in their suspensory quadrupedal locomotion[13], a mode of locomotion which is advanced in Megachiropteran bats like *Rousettus* relative to Microchiropteran species[14]. Compared with other species, *Rousettus* has an exceptional degree of forelimb and hindlimb coactivation from stimulation of individual sites in motor cortex. This coactivation of forelimb and hindlimb muscles from overlapping cortical areas may support the coordinated movements involved in flight aerodynamics[10]. Finally, we found that bilateral forelimb movements were concentrated in M1 and rostral regions of S1, similar to recent findings of bilateral forelimb movements in rostral portions of the neocortex in rats (primarily M1[7]).

In contrast to the coupling of forelimb movements with those of the hindlimb, our study found an exceptional number of evoked hindlimb movements that were independent of forelimb coactivation, and that were evoked over a large portion of cortex (especially in medial S1 and area 1/2). Given that the hindlimb plays a central role in determining the tension of the wing membrane during flight,[15] this magnification of the hindlimb representation may be an adaptation to facilitate motor control of the wing tension and shape. Finally, we found that movements of the wing membranes were elicited from a few sites in area 1/2 (Figure 1; caudal membranes) and S1/M1 (Figure S2: 18–99; rostral

membranes). Here we provide evidence for cortical control of wing membrane musculature in the Egyptian fruit bat, distributed across M1, S1, and area 1/2. Taken together, our data shows that a distributed network of cortical areas contributes to the coordinated control of muscles that are involved in self-propelled flight.

While flight is common to all bats, *Rousettus* is a rare genus of megabat that echolocates, using tongue-clicks (rather than the larynx, as in most microbats) to generate active sonar.[1] Interestingly, *Rousettus* rapidly produces directional sonar beams without changing the position of the head or the shape of the mouth, suggesting precise motor control of the tongue in the production of sonar clicks.[2] Here, we show that stimulation of a large proportion of cortex in *Rousettus* elicits movements of the tongue (~42% of S1+M1), and that distinct regions of M1 and S1 generate movements of particular tongue regions (proximal vs. distal) as well as full extensions of the tongue. While comparisons with previous studies of motor cortex in other mammals are complicated by methodological differences (e.g. the lateral extent of stimulation), we measured the size of tongue representations from studies in several other species in which similar ICMS procedures were utilized (Table 1). Studies from our lab using similar methods found the tongue movement representation occupied ~8% of M1 in macaque monkeys,[6] ~2% of M1 in capuchin monkeys,[12] and ~28% of M1 in tree shrews[17] (see Methods). A recent study in our lab focusing on complex forelimb and hindlimb movement types failed to elicit tongue movements in rats, but the tongue region was not actively explored.[7] However, a classic study[16] found that ~26% of rat cortex (including S1 and M1) produced tongue movements. Even the largest tongue representations previously reported in M1 (~28% in tree shrew, 26% in rat) are substantially smaller than the 43% we observed in *Rousettus*, given these species' similar brain sizes (*Tupaia*: 3.15 g;[18] *Rattus*: 2.38 g;[18] *Rousettus*: 1.89 g (current study]) and the regular scaling of S1 with brain size.[19] Regardless of the technique used, compared with other species, the movement representation of the tongue in *Rousettus* is exceptionally large (Table 1).

An established feature of organization of sensory cortex is the magnification of behaviorally relevant sensory surfaces, such as the electrosensitive bill of the platypus[3], the nose of the star-nosed mole,[4] or teeth in naked mole rat.[5] In the current study, we describe a complementary form of cortical magnification in the tongue motor cortex of *Rousettus*. Our data suggests an extreme example of this organizational feature, with an enlarged representation of the tongue in regions of the neocortex involved in motor control (e.g. S1, M1)(Figure 3A). This magnification of the tongue motor representation (Figure 3B) is comparable to specializations of the neocortex for manual dexterity in primates (Figure 3C) and motor substrates for language in humans (Figure 3D). The size and differentiation of tongue motor representations are clearly extreme in *Rousettus*, and their unique lingual form of echolocation is an attractive hypothesis to explain these cortical adaptations. However, given that control of the tongue is central to a range of mammalian behaviors[20] including mastication, further studies of motor cortex in non-echolocating megabats are necessary to determine whether this unique cortical phenotype reflects the lingual form of echolocation unique to this genus, or frugivorous mastication in megabats generally.

Although cortical magnification of behaviorally relevant sensory surfaces appears to be a general feature of the neocortex, the magnification of motor representations differs from the magnification of body part representations in sensory cortex in important ways. Somatosensory cortex (e.g. S1) is organized in a relatively tight somatotopic fashion relative to the contralateral sensory epithelium, but the organization of motor cortex is less topographic relative to body surfaces or muscle locations. Instead, motor cortex appears to be organized around muscle synergies that support species-unique behaviors.[6,12, 20–24] If we compare individuals within a species, motor maps exhibit more variability than somatosensory maps do. This is what we should expect if the muscle coactivations involved in movement – built over the lifetime – are more variable than the sensory epithelium, which is more constant within a given species.

How does motor cortex coevolve with body morphology, especially in species with exceptional peripheral adaptations, such as wings? Given that the organization of sensorimotor cortex is sensitive to changes in peripheral morphology during development,[25–28] a central question is the extent to which differences in motor cortex organization are due to genes associated with cortical arealization or alterations in the development of peripheral body regions. In bats, it is likely that motor representations of the body have coevolved with changes to peripheral morphogenesis, such as the genetic programs responsible for the elongation of forelimb bones that constitute the wing, and an inhibition of bone morphogenic proteins that normally reduce interdigit membranes, to name a few.[29–32] Ultimately, the remarkable phenotypic variability of mammalian behavior involves a complex coevolution of motor representations in the brain and body morphologies that allow for specialized forms of movement, including echolocation and flight.

STAR Methods

Resource Availability

Lead Contact—Further information and requests for resources should be directed to, and will be fulfilled by, the lead contact, Leah Krubitzer (lakrubitzer@ucdavis.edu).

Materials Availability—This study did not generate any new reagents or materials.

Data and Code Availability—This study did not generate any new code or datasets. Voronoi tessellations were produced using a plugin for Adobe Illustrator (https://github.com/ff6347/Illustrator-Javascript-Voronoi).

Experimental Model and Subject Details

Nine adult Egyptian fruit bats (*Rousettus aegyptiacus*)(4 females, mean body weight 115 ± 7 g; 5 males, mean body weight 113 ± 29 g) were used to characterize movements elicited from intracortical microstimulation (ICMS). Two cases with particularly high-density maps are presented in Figure 1, with abbreviations listed in Table S1. Threshold data for these cases are shown in Figure S2, and summarized in Table S2. Three additional cases are shown in Figure S3. Animals were directly transported from a colony at UC Berkeley to UC Davis. All transportation procedures were approved by both UC Berkeley and UC Davis;

all experimental procedures were approved by UC Davis IACUC, and conform to NIH Guidelines.

Method Details

Surgical Procedures—Anesthetic induction was achieved by a combination of ketamine hydrochloride (30 mg/kg; IM) and xylazine (4 mg/kg, IM). Maintenance doses of ketamine (8–25%) and xylazine (10–25%) were administered through the remainder of the experiment as needed. Respiration rate, body temperature, eye-blink, and muscle tone were monitored throughout each experiment to ensure a steady level of anesthesia. A combination of lactated ringer's solution (0.8 mL) and dextrose (0.2 mL) was administered every 2–4 h.

Animals were placed into a stereotaxic frame with ear bars coated in 5% lidocaine cream. An injection of lidocaine (2%) was injected subcutaneously along the midline of the scalp. The skin and temporal muscles were retracted bilaterally to expose the skull. A large craniotomy in either the left (n=7) or right hemisphere (n=2) was made, and the dura was retracted. To prevent desiccation, silicone fluid was applied to the cortical surface. Two small screws were placed into the skull contralateral to the craniotomy to secure the head for stimulation.

Animals were transferred to a custom-built platform designed to support the ventral torso while allowing the forelimbs, hindlimbs, and wing membranes to hang freely at the sides. A head post was secured to the skull using dental acrylic applied to the skull screws, then secured to a stereotaxic frame.

ICMS Mapping—Biphasic stimulation pulses were generated using a Grass S88 stimulator and two stimulation isolation units (SIUs), and were delivered using a low impedance microelectrode (0.1 MΩ). Stimulation consisted of long (500 ms) trains of biphasic pulses (a 0.2 ms positive phase followed by a 0.2 ms negative phase) delivered at 200 Hz. Electrodes were lowered into the cortex to a depth of 1600 μm when the electrode was inserted perpendicular to the cortical surface, and up to 1800 μm when inserted at an angle. Current amplitude of stimulation was measured using the voltage drop across a 10 kΩ resistor in series with the return lead of the SIUs. This metric was used to monitor the integrity of the electrode throughout the experiment in real time; electrodes were replaced as needed.

Stimulation was applied in individual bursts of 500 ms, separated by ~5–10 seconds between stimulations. This period is used to record the movements elicited from each individual stimulation site, and to prevent overstimulation of a given site (including habituation effects). In general, we aim to fully characterize each site, including movement types and thresholds, using the smallest number of possible individual stimulations. If movements habituate after only one or two stimulations, they are not recorded for a particular site.

Movements elicited from ICMS were confirmed and recorded by at least two researchers, including the body parts involved and the nature of the movement. All movements observed up to 300 μA were described, and stimulation thresholds for LT-ICMS were measured as the lowest current to evoke a movement. At each site, higher currents were initially applied to characterize movement types, followed by progressively lower currents to determine

movement thresholds. At sites of interest, movements were recorded from two different angles (Sanyo Xacti VPC-HD2000A, 1920 × 1080 resolution, 60 fps). At select sites (e.g. membrane sites), movements up to 500 μA were recorded. An LED connected to the stimulator was included in each video frame and illuminated during stimulation trains. A scale was included in the video frame for movement analysis. Still frames were extracted from video files using the VLC media player, and stacked as layers in Adobe Illustrator in order to trace movement trajectories during stimulation. For tongue movements, the most prevalent region of movement was at the distal end of the tongue. Against this common pattern, we noted any movements that occurred in deeper regions, and used a simple classification system (distal, middle, proximal) to characterize these.

Original studies using LT-ICMS were done in awake behaving monkeys by the Graziano lab.[19] In motor cortex they elicited different types of ethologically relevant movements such as grasping, and hand to mouth behaviors. However, these types of studies are limited in the extent of cortex that can explored in a single animal. Similar but not identical types of movements have also been elicited in anesthetized animals including primates (e.g. reaching, grasping, hand to mouth).[6,12,17,19,20] Using an anesthetized preparation allows us to explore a large region of cortex including motor, somatosensory and posterior parietal areas, and define the full extent of cortex involved in motor control.

Histological Processing—Animals were euthanized with a lethal dose of sodium pentobarbital (>390 mg/kg) and transcardially perfused with saline followed by 2% paraformaldehyde (PFA). After perfusion, the brain was extracted from the skull. In six cases, the neocortex was then separated from the brainstem and thalamus, manually flattened, post-fixed in 4% PFA under a glass slide for 0.5–1.5 h, and left in 30% sucrose in phosphate buffer overnight for cryoprotection. The neocortex was then sectioned on a freezing microtome at a thickness of 50–60 μm. In three cases in which the brain was sectioned in coronal or horizontal planes, the whole brain was post-fixed in 4% PFA and left overnight in 30% sucrose in phosphate buffer. The whole brain was then sectioned on a freezing microtome at a thickness of 30 μm (horizontal) or 50–60 μm (coronal). Photographs of the block face were taken between each section (Nikon D5200 with a Nikkor 55–200 mm lens and Raynox DCR-250 macroscopic conversion lens) to allow for 3D reconstruction of the whole brain (e.g. Figure S1K). Flattened cortex was stained in alternating series for myelin and cytochrome oxidase (CO; Figure S1, G to H). Coronal and horizontal sections were stained in alternating series for myelin, CO, Nissl, vesicular glutamate 2 (VGLUT2; not shown), or acetylcholinesterase (AchE; not shown)(Figure S1, I to O).

Quantification and Statistical Analysis

Alignment of Functional and Histological Data—Methods for combining histological and ICMS data have been described previously[7] and are detailed in Figure S1. During the experiment, a high-resolution photograph was taken of the brain and used to record the location of electrode sites and fiduciary probes (Figure S1C). These photographs were compared with stained tissue sections, and manually aligned in Adobe Photoshop using blood vessels, electrode tracts, and morphology as landmarks for registration.

In flattened cases, electrode locations were identified on stained tissue by matching surface vasculature in superficial CO sections (Figure S1E) with electrode locations marked on a photograph of the brain surface (Figure S1C). Cortical field boundaries were identified from CO and myelin stains (Figure S1G, H). In coronal and horizontal cases, electrode sites marked on surface photographs (Figure S1J) were integrated with 3D reconstructions from block-face images (Figure S1K). Cortical field boundaries were determined from stained sections (Figure S1, M to O), applied to 3D reconstructions, and directly integrated with experimental data from surface maps (Figure S1J).

Motor maps were produced by applying a Voronoi tessellation script to electrode sites in Adobe Illustrator (https://github.com/ff6347/Illustrator-Javascript-Voronoi) which generates a polygon comprising all cortex adjacent to an electrode site.[7] Each polygon was assigned a color or combination of colors, according to the body part movements elicited from stimulation at that site. Maps indicate all movements elicited following stimulation up to 300 μA.

Quantification of Movement Types—The surface area of individual movement-types representations was measured relative to a scale bar in Adobe Photoshop. All measurements were taken in cases prepared with flattened sections. Measurements of fore- and hindlimb movements in rats from an earlier study[7] were made from two representative cases (15–65 and 15–63, shown in Figure 4 of that paper). Measurements of tongue representation proportions are shown in Table S3, and summarized in Table 1. For each species, measurements were made from LT-ICMS cases relative to scale bars provided for each figure. The sources and case numbers for each case are described in Table S3. Tongue region proportions are a ratio of tongue-elicitation surface area vs. the whole surface area of elicited movements within a given region (M1, S1, or M1+S1).

Supplementary Material

Refer to Web version on PubMed Central for supplementary material.

Acknowledgements

We thank Carly Jones, Deepa Ramamurthy, and Alyssa Sanchez for assistance with experiments, Cynthia Weller for assistance with histology, and Yuka Minton for assistance with animal transport. Funding sources include the McDonnell Foundation 220020516 (L.K.); National Eye Institute 5T32EY015387-15 (A.C.H.); Banting Research Foundation Discovery Award (D.F.C.); NIH DP2-DC016163 (M.M.Y.); NIMH 1-R01MH25387-01 (M.M.Y.); New York Stem Cell Foundation NYSCF-R-NI40 (M.M.Y.); Alfred P. Sloan Foundation FG-2017-9646 (M.M.Y.); Brain Research Foundation BRFSG-2017-09 (M.M.Y.); Packard Fellowship 2017-66825 (M.M.Y.); Klingenstein Simons Fellowship (M.M.Y.); Human Frontiers Science Program (M.M.Y.); Pew Charitable Trust 00029645 (M.M.Y.); McKnight Foundation (M.M.Y.); Dana Foundation (M.M.Y.); New York Stem Cell Foundation – Robertson Investigator (M.M.Y.).

References

1. Yovel Y, Geva-Sagiv M, and Ulanovsky N (2011). Click-based echolocation in bats: not so primitive after all. J. Comp. Physiol 197, 515–530. [PubMed: 21465138]
2. Lee W-J, Falk B, Chiu C, Krishnan A, Arbour JH, and Moss CF (2017). Tongue-driven sonar beam steering by a lingual-echolocating fruit bat. PLOS Biol. 15, e2003148. [PubMed: 29244805]

3. Krubitzer L, Manger P, Pettigrew J, and Calford M (1995). Organization of somatosensory cortex in monotremes: in search of the prototypical plan. J. Comp. Neurol 351, 261–306. [PubMed: 7699113]
4. Catania KC, and Kaas JH (1997). Somatosensory fovea in the star-nosed mole: behavioral use of the star in relation to innervation patterns and cortical representation. J. Comp. Neurol 387, 215–233. [PubMed: 9336224]
5. Catania KC, and Remple MS (2002). Somatosensory cortex dominated by the representation of teeth in the naked mole-rat brain. Proc. Natl. Acad. Sci. U.S.A 99, 5692–5697. [PubMed: 11943853]
6. Baldwin MKL, Cooke DF, Goldring AB, and Krubitzer L (2018). Representations of fine digit movements in posterior and anterior parietal cortex revealed using long-train intracortical microstimulation in macaque monkeys. Cereb. Cortex 28, 4244–4263. [PubMed: 29136133]
7. Halley AC, Baldwin MKL, Cooke DF, Englund M, and Krubitzer L (2020). Distributed motor control of limb movements in rat motor and somatosensory cortex: The sensorimotor amalgam revisited. Cereb. Cortex 30, 6296–6312. [PubMed: 32691053]
8. Krubitzer LA, Calford MB, and Schmid LM (1993). Connections of somatosensory cortex in megachiropteran bats: The evolution of cortical fields in mammals. J. Comp. Neurol 327, 473–506. [PubMed: 8440777]
9. Song A, Tian X, Israeli E, Galvao R, Bishop K, Swartz S, and Breuer K (2008). Aeromechanics of membrane wings with implications for animal flight. A.I.A.A. Journal 46, 2096–2106.
10. Sterbing-D'Angelo S, Chadha M, Chiu C, Falk B, Xian W, Barcelo J, Zook JM, and Moss CF (2011). Bat wing sensors support flight control. Proc. Natl. Acad. Sci. U.S.A 108, 11291–11296. [PubMed: 21690408]
11. Krubitzer L, Clarey JC, Tweedale and R, and Calford MB (1998). Interhemispheric connections of somatosensory cortex in the flying fox. J. Comp. Neurol 402, 538–559. [PubMed: 9862325]
12. Mayer A, Baldwin MKL, Cooke DF, Lima BR, Padberg J, Lewenfus G, Franca JG, and Krubitzer L (2019). The multiple representations of complex digit movements in primary motor cortex form the building blocks for complex grip types in capuchin monkeys. J. Neurosci 39, 6684–6695. [PubMed: 31235643]
13. Granatosky MC (2018). Forelimb and hindlimb loading patterns during quadrupedal locomotion in the large flying fox (Pteropus vampyrus) and common vampire bat (Desmodus rotundus). J. Zool 305, 63–72.
14. Adams RA, and Carter RT (2017). Megachiropteran bats profoundly unique from microchiropterans in climbing and walking locomotion: Evolutionary implications. PLOS ONE 12, e0185634. [PubMed: 28957404]
15. Cheney JA, Konow N, Middleton KM, Breuer KS, Roberts TJ, Giblin EL, and Swartz SM (2014). Membrane muscle function in the compliant wings of bats. Bioinspir. Biomim 9, 025007. [PubMed: 24855069]
16. Neafsey EJ, Bold EL, Haas G, Hurley-Gius KM, Quirk G, Sievert CF, and Terreberry RR (1986). The organization of the rat motor cortex: A microstimulation mapping study. Br. Res. Rev 11, 77–96.
17. Baldwin MKL, Cooke DF, Krubitzer L (2017). Intracortical microstimulation maps of motor, somatosensory, and posterior parietal cortex in tree shrews (Tupaia belangeri) reveal complex movement representations. Cereb. Cortex 27, 1439–1456. [PubMed: 26759478]
18. Sacher GA, and Staffeldt EF (1974). Relation of gestation time to brain weight for placental mammals: Implications for the theory of vertebrate growth. Amer. Nat 108, 593–615.
19. Kaskan PM, Franco ECS, Yamada ES, de Lima Silveira LC, Darlington RB, and Finlay BL (2005). Peripheral variability and central constancy in mammalian visual system evolution. Proc. R. Soc. B 272, 91–100.
20. Bollu T, Ito BS, Whitehead SC, Kardon B, Redd J, Liu MH, and Goldberg JH (2021). Cortex-dependent corrections as the tongue reaches for and misses targets. Nature 594, 82–87. [PubMed: 34012117]
21. Graziano MSA, Taylor CSR, and Moore T (2002). Complex movements evoked by microstimulation of precentral cortex. Neuron 34, 841–851. [PubMed: 12062029]

22. Stepniewska I, Fang P-C, and Kaas JH (2005). Microstimulation reveals specialized subregions for different complex movements in posterior parietal cortex of prosimian galagos. Proc. Natl. Acad. Sci. U.S.A 102, 4878–4883. [PubMed: 15772167]

23. Graziano MSA, and Cooke DF (2006). Parieto-frontal interactions, personal space, and defensive behavior. Neuropsychologia 44, 2621–2635. [PubMed: 17128446]

24. Brown AR, and Teskey GC (2014). Motor cortex is functionally organized as a set of spatially distinct representations for complex movements. J. Neurosci 34, 13574–13585. [PubMed: 25297087]

25. Merzenich MM et al. (1983). Topographic reorganization of somatosensory cortical areas 3b and 1 in adult monkeys following restricted deafferentation. Neurosci. 8, 33–55.

26. Florence SL, and Kaas JH (1995). Large-scale reorganization at multiple levels of the somatosensory pathway follows therapeutic amputation of the hand in monkeys. J. Neurosci 15, 8083–8095. [PubMed: 8613744]

27. Wu CW, and Kaas JH (1999) Reorganization in primary motor cortex of primates with long-standing therapeutic amputations. J. Neurosci 19, 7679–7697. [PubMed: 10460274]

28. Qi H-X, Stepniewska I, and Kaas JH (2000). Reorganization of primary motor cortex in adult macaque monkeys with long-standing amputations. J. Neurophysiol 84, 2133–2147. [PubMed: 11024101]

29. Sears KE, Behringer RR, Rasweiler JJ, and Niswander LA (2006). Development of bat flight: Morphologic and molecular evolution of bat wing digits. Proc. Natl. Acad. Sci. U.S.A 103, 6581–6586. [PubMed: 16618938]

30. Weatherbee SD, Behringer RR, Rasweiler JJ, and Niswander LA (2006). Interdigital webbing retention in bat wings illustrates genetic changes underlying amniote limb diversification. Proc. Natl. Acad. Sci. U.S.A 103, 15103–15107. [PubMed: 17015842]

31. Tokita M, Abe T, and Suzuki K (2012). The developmental basis of bat wing muscle. Nat. Commun 3, 1302. [PubMed: 23250432]

32. Eckalbar WL, Schlebusch SA, Mason MK, Gill Z, Parker AV, Booker BM, Nishizaki S, Muswamba-Nday C, Terhune E, Nevonen KA, et al. (2016). Transcriptomic and epigenomic characterization of the developing bat wing. Nat. Genet 48, 528–536. [PubMed: 27019111]

33. Henry P-G, Adrany G, Deelchand D, Gruetter R, Marjanska M, Oz G, Seaquist ER, Shestov A, Ugurbil K (2006). In vivo 13C NMR spectroscopy and metabolic modeling in the brain: a practical perspective. Magn. Reson. Imaging 24, 527–539. [PubMed: 16677959]

Highlights

- The first motor map of any bat species using intracortical microstimulation
- *Rousettus*, a lingual echolocating bat, has an enlarged tongue motor representation
- Forelimb movements are usually coupled with hindlimb movements
- Motor organization is consistent with adaptations for flight and echolocation

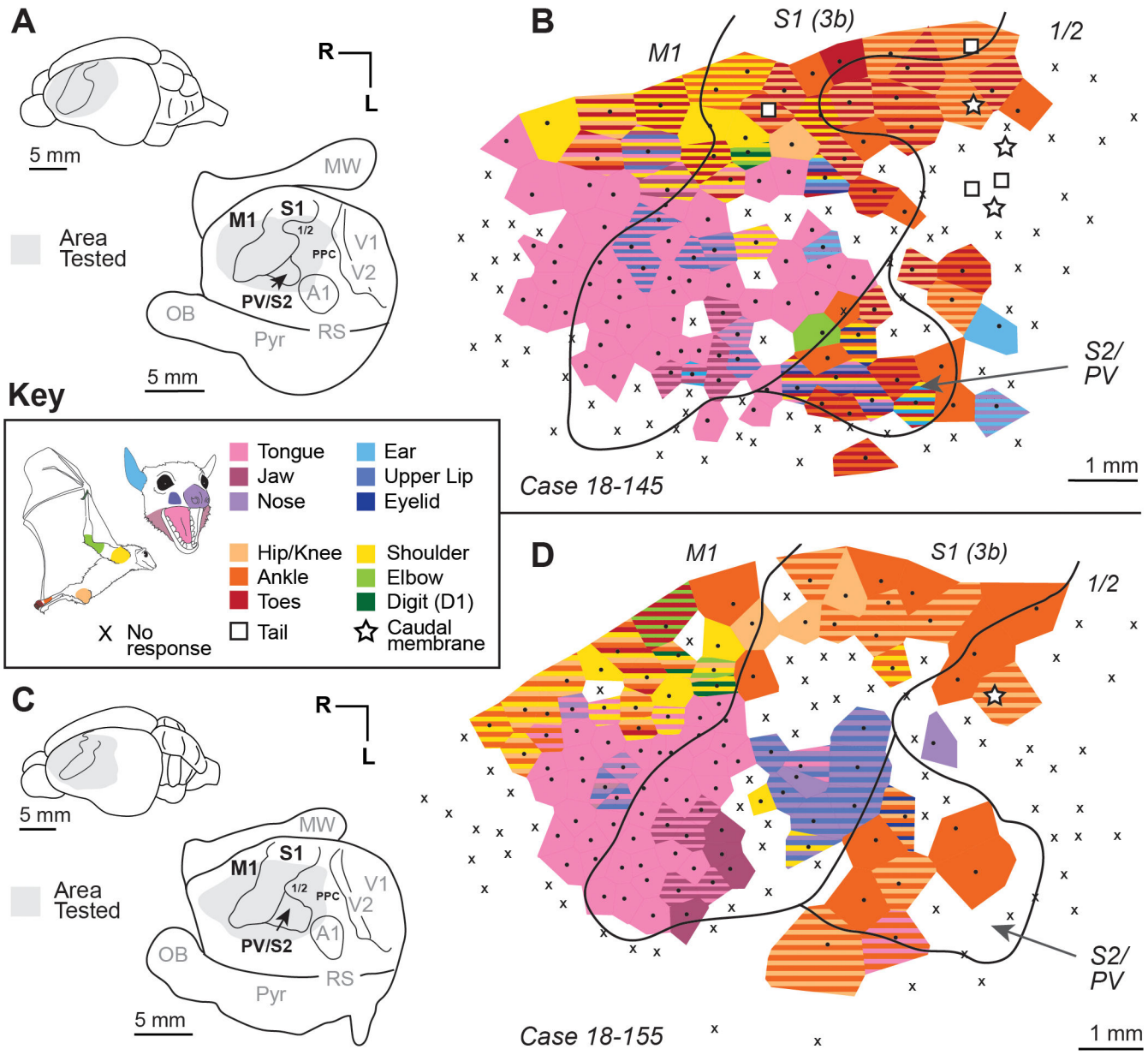

Figure 1. Movement maps in two bats.

(A) Lateral and flattened views of the left hemisphere in case 18–145. Cortical field boundaries are indicated by black lines, and the region mapped using long-train ICMS is shown in grey. **(B)** A map of the movements elicited, corresponding to the grey regions shown in (A). Black dots indicate stimulation sites from which movements were elicited and grey X's indicate sites where no movements were elicited up to 300 μA. Polygon color indicates the body parts from which movements were elicited. Striped colors indicate multiple body part movements at given site. **(C)** Lateral and flattened views of case 18–155, as above. **(D)** Movement map for case 18–155, as above. See Table S1 for abbreviations. Tail and membrane sites outside of colored polygons were observed at thresholds >300 μA. See Table S1 for abbreviations. See also Figure S2, Table S2.

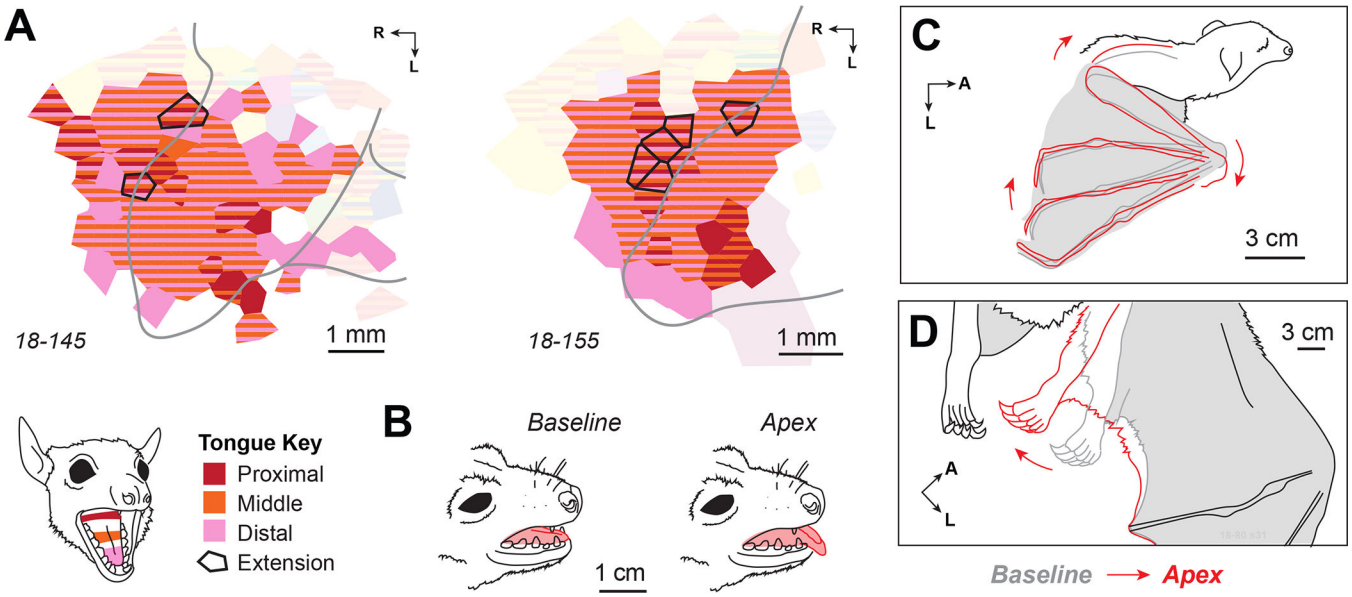

Figure 2. Example movements of the tongue, forelimb, and hindlimb.

(A) Movements of the tongue can be subdivided into proximal, middle, and distal subregions. While most sites elicited movements of the distal and/or middle tongue, clusters of sites elicited movements in the proximal tongue. Black outlines indicate sites that elicited full extensions of the tongue. **(B)** Example of an extension of the tongue. **(C)** A typical forelimb site, eliciting movement of the entire wing originating from the shoulder. Grey outlines indicate the baseline position of the limb, and red outlines indicate the limb position at the apex of elicited movement. **(D)** Example movement of the hindlimb moving medially, affecting the camber of the wing. Color conventions as in (C). See Figure 1 for full maps of cases shown in 2A.

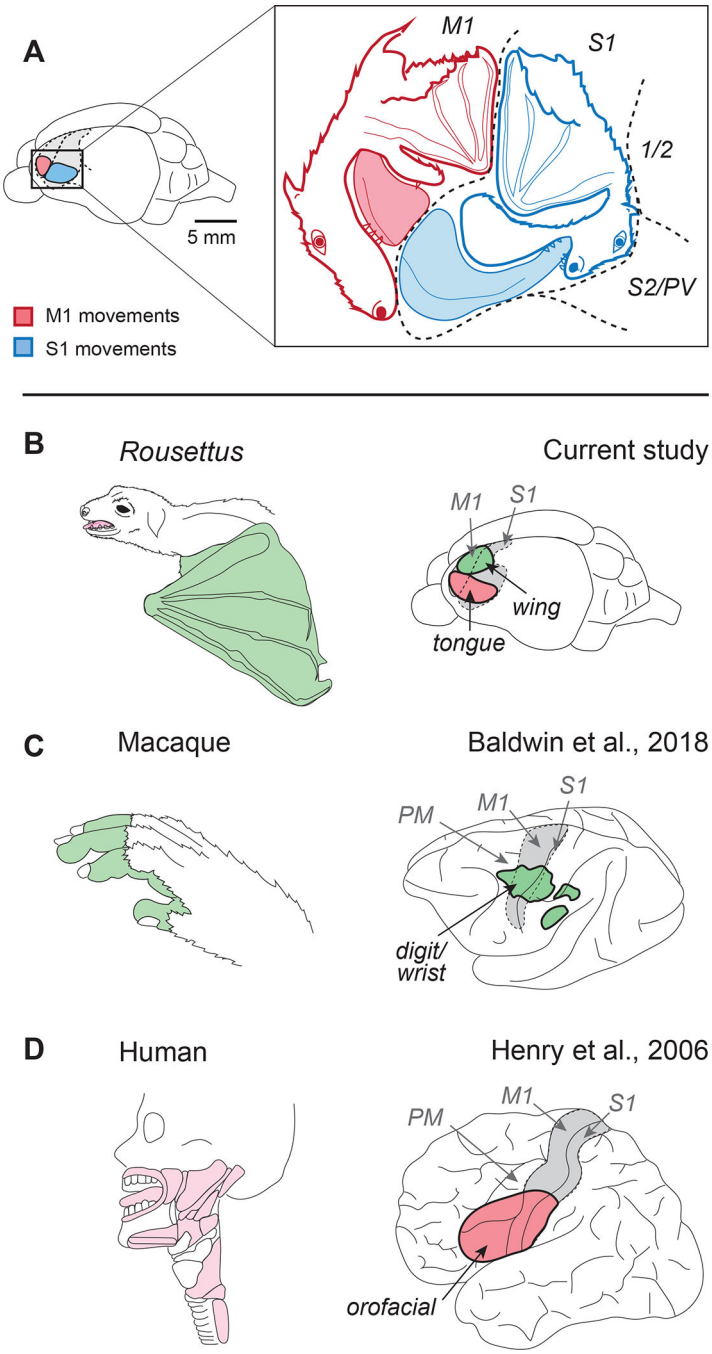

Figure 3. The magnification of cortical sensorimotor representations to support behavioral specializations in mammals.

(A) In the Egyptian fruit bat, intracortical microstimulation elicits movements of the tongue from a large portion of both primary motor (M1) and primary somatosensory cortex (S1). This "batunculus" diagram approximates the enlarged representation of tongue, hindlimb, and forelimb movements elicited with ICMS. Our findings in *Rousettus* emphasize how representations in motor cortex coevolve with specializations in peripheral morphology and behavior. **(B)** In fruit bats, movements of the tongue (purple) and wing (green) occupy

a large region of cortex to support echolocation and flight propulsion. **(C)** In rhesus monkeys, an enlarged region of cortex is devoted to movements of the wrist and digits, an adaptation that supports manual dexterity in many primate species, including humans. **(D)** The production of human language requires the use of diverse muscle groups, including classic “language areas” of the brain (e.g. Broca’s area). Subregions of somatosensory, motor, and premotor cortex are central to the production of human speech. (C) and (D) adapted from Baldwin et al.[6] and Henry et al.[33] See Table S1 for abbreviations.

Table 1.

Average size of tongue movement representations in M1 and S1 in five species.

	All Movements (mm^2)			Tongue Movements (mm^2)			% Tongue Movements		
Sp. (case #)	**S1+M1**	**S1**	**M1**	**S1+M1**	**S1**	**M1**	**S1+M1**	**S1**	**M1**
Bat (5)	14.2	9.2	5.0	6.3	4.1	2.3	41.5%	40.9%	43.7%
Capuchin (4)	-	-	128.89	-	-	3.07	-	-	2.3%
Macaque (2)	-	-	107.54	-	-	7.98	-	-	8.3%
TrShrew (6)	15.69	10.42	5.27	2.38	0.93	1.45	16.0%	8.9%	28.0%
Rat (Neafsey)	61.0	-	-	16.0	-	-	26.2%	-	-

In *Rousettus,* the tongue has an exceptionally large representation relative to other movement types in both S1 and M1. The measures in this study are similar to those used for capuchin, macaque, tree shrew, and rat. S1 is embedded in the central sulcus in capuchin and macaque, so could not be measured. Rat measures are taken from a classic study by Neafsey et al.[16] Sources and methods are described in STAR Methods. See Table S3 for measurements of individual cases.

KEY RESOURCES TABLE

REAGENT or RESOURCE	SOURCE	IDENTIFIER
Chemicals, Peptides, and Recombinant Proteins		
Acetic Anhydride	Fisher	A10-4
Acetic Acid	Fisher	A38-212
AgNO3 (Silver Nitrate)	Sigma	209139
NH4NO3 (Ammonium Nitrate)	Fisher	A676-212
Cytochrome C	Sigma	C2506
Na2CO3 (Sodium Carbonate)	Fisher	S263-500
Tungstosilicic Acid	Sigma	T2786
Formaldehyde (37%)	Fisher	F79P-4
NaThio SO4	Fisher	S446-500
KFeCN	MP Biomedicals	152559
Chloroform	VWR	BDH1109-4LG
EtOH	Koptec	TX89125-172
Cresyl violet	Sigma	C5042-10G
Catalase	Sigma	C9322
Xylenes	Fisher	X5-4
DAB	Sigma	D5637
Paraformalhyde prills	EMS	19200
Pyradine	Fisher	P368-4
Experimental Models: Organisms/Strains		
Rousettus aegyptiacus (Egyptian fruit bat)	UC Berkeley	
Software and Algorithms		
Photoshop	Adobe	
Spike2	Cambridge Electronic Design Limited	
Javascript Voronoi (AI Plugin)	MIT License	
Illustrator	Adobe	